

# Overall momentum balance and redistribution of the lost energy in asymmetric dijet events in 2.76 ATeV Pb-Pb collisions with a multi-phase transport model

Zhan Gao,<sup>1</sup> Guo-Liang Ma,<sup>2</sup> Guang-You Qin,<sup>1</sup> and Han-Zhong Zhang<sup>1</sup>

<sup>1</sup>*Key Laboratory of Quark and Lepton Physics (MOE) and Institute of Particle Physics,  
Central China Normal University, Wuhan 430079, China*

<sup>2</sup>*Shanghai Institute of Applied Physics, Chinese Academy of Sciences, Shanghai 201800, China*  
(Dated: May 30, 2019)

The overall transverse momentum balance and the redistribution of the lost energy from hard jets for asymmetric dijet events in PbPb collisions at 2.76 ATeV at the LHC is studied within A Multi-Phase Transport (AMPT) model. A detailed analysis is performed for the projected transverse momentum  $\langle p_T^\parallel \rangle$  contributed from the final charged hadrons carrying different transverse momenta and emitted from different angular directions. We find that the transverse momentum projection  $\langle p_T^\parallel \rangle$  in the leading jet direction is mainly contributed by hard hadrons ( $p_T > 8.0$  GeV/c) in both peripheral and central PbPb collisions, while the opposite direction in central collisions is dominated by soft hadrons ( $p_T = 0.5\text{--}2.0$  GeV/c). The study of in-cone and out-of-cone contributions to  $\langle p_T^\parallel \rangle$  shows that these soft hadrons are mostly emitted at large angles away from the dijet axis. Our numerical result is qualitatively consistent with the CMS measurements, which indicates that in the AMPT model, a large amount of the lost energy from hard jets occurred in the partonic stage is transported by elastic collisions to soft partons (hadrons) at large angles. Future studies including also inelastic processes should be helpful in understanding the overestimation of the magnitudes of in-cone and out-of-cone imbalances from our AMPT calculations, and shed light on different roles played by radiative and collisional processes in the redistribution of the lost energy from hard jets.

## I. INTRODUCTION

Jet quenching is one of the most important evidences for the formation of the hot and dense quark-gluon plasma (QGP) in high-energy heavy-ion collisions [1, 2]. It originates from the energy loss experienced by the hard partonic jets initially produced from early scatterings as they traverse and interact with the highly excited nuclear matter created in these energetic collisions. The picture of parton energy loss and jet quenching has been confirmed by a wealth of experimental evidences observed at the Relativistic Heavy-Ion Collider (RHIC) and the Large Hadron Collider (LHC), such as the suppression of large transverse momentum hadron production [3–7], and the strong modification of dihadron and photon-hadron transverse momenta and azimuthal angle correlations [8–11], in central nucleus-nucleus collisions as compared to elementary nucleon-nucleon collisions. Various theoretical and phenomenological models have been developed to explain these jet modification phenomena [12–26], and shown that jet energy loss is a combinational effect from elastic and inelastic interactions between the propagating hard partons and the constituents of the hot and dense QGP matter.

In recent years, much attention has been devoted to fully reconstructed jet observables in relativistic heavy-ion collisions. As full jets include the contributions from both leading and subleading fragments of the parton showers, they are expected to provide more detailed information than hadronic observables on the interaction between jet and medium. Various full jet observables have been studied in heavy-ion experiments at RHIC and the LHC, e.g., single inclusive full jet spectra [27–31], the transverse momentum asymmetry distributions and an-

gular correlations for dijet and photon-jet events [32–35], and the internal structures of the full jets [36–38]. In order to understand the observed nuclear modifications of full jet production and structure, it is required to develop theoretical models and calculations that include the effect of the medium on both leading and subleading partons of the full jets [39–57]. The comparisons between theories and experiments have demonstrated that full jets may experience a significant amount of energy loss as well when they propagate through the hot and dense nuclear matter, and the distribution of the energy and momentum inside full jets may also be strongly modified by the interaction with the medium constituents.

As we know, when hard partonic jets propagate through the hot and dense QGP matter, they not only lose energy due to jet-medium interaction, but also induce medium excitations [58–62]. In particular, the energy and momentum lost from hard jets are deposited into the medium, which may modify the subsequent medium evolution and manifest in the final-state hadron distributions and correlations. Therefore, it is of great interest to investigate the fate of the lost energy from the jets, e.g., how it evolves with the dynamical medium and where it goes. This is the motivation of our work. We study the redistribution of the lost energy from jets following the CMS Collaboration, and calculate the so-called projected transverse momentum  $\langle p_T^\parallel \rangle$  for asymmetric dijet events within the framework of A Multi-Phase Transport Model (AMPT) [63]. It is worth noting that in Ref. [64] such observable has been studied with a (3+1)-dimensional hydrodynamic model (using a simplified energy deposition profile). Here we simulate both jet propagation and medium evolution together simultaneously with the AMPT model, and perform a detailed

analysis for the various contributions to  $\langle p_T^\parallel \rangle$  from the final state hadrons carrying different transverse momenta and emitted from different angular directions with respect to the dijet propagation direction. Our simulation results are qualitatively consistent with the CMS observation and show that a large amount of the deposited energy and momentum by the hard partonic jets are then transported by elastic collisions (in the AMPT model) and finally carried by the soft hadrons emitted at large angles away from the dijet propagation direction.

The paper is organized as follows. In Sec. II, we provide a brief introduction to the AMPT model and the corresponding settings used in our studies. The numerical results on the transverse momentum projection  $\langle p_T^\parallel \rangle$  for asymmetric dijet events are presented and discussed in detail in Sec. III. Sec. IV contains the summary.

## II. THE AMPT MODEL

In this work, we use the AMPT model with string melting mechanism [63], which has provided good descriptions of various soft bulk observables at the LHC energies [65]. In addition, the AMPT model with a triggered dijet can also describe many aspects of the full reconstructed jet observables, such as the transverse momentum  $p_T$  asymmetry of dijet or photon-jet events [47, 66], jet fragmentation function [67], jet shape function [68] and jet anisotropy parameter [69].

In the AMPT model, there are four main stages in high-energy heavy-ion collisions: the initial condition, parton cascade, hadronization, and hadronic rescatterings. (i) The initial condition of the AMPT model is obtained from HIJING model [70, 71], which consists of the spatial and momentum information of minijet partons and soft string excitations. In order to increase the simulation efficiency for studying jet quenching phenomena, the production of a dijet is triggered with the help of the HIJING model jet triggering technique [70, 71], which produces a triggered dijet with a specified  $p_T$  in

each event. Several hard QCD processes are taken into account in the triggered dijet production:  $q_1 q_2 \rightarrow q_1 q_2$ ,  $q_1 \bar{q}_1 \rightarrow q_2 \bar{q}_2$ ,  $q \bar{q} \rightarrow g g$ ,  $q g \rightarrow q g$ ,  $g g \rightarrow q \bar{q}$ , and  $g g \rightarrow g g$ . In the AMPT model, all initial-state and final-state radiation corrections are included, therefore, a high- $p_T$  primary parton evolves into a full jet shower parton with lower virtualities. Then the triggered jets together with the minijets and soft string excitations are fragmented into hadrons according to the Lund string fragmentation [72]. All hadrons are then converted to quarks according to the flavor and spin structures of their valence quarks, forming a quark and anti-quark plasma. (ii) The evolution of partonic plasma is simulated by Zhang's parton cascade (ZPC) model [73], which describes elastic partonic collisions among the medium partons and jet partons. The interaction strength of the elastic collisions is controlled by the partonic cross section, which is further determined by the value of the strong coupling constant and the Debye screening mass. (iii) When the collisions of all partons stop, the AMPT model hadronizes partons via a simple coalescence model which combines two nearest quarks into a meson and three nearest quarks into a baryon. The triggered dijet is also converted to a hadronic dijet via the coalescence mechanism. (iv) The dynamics of the subsequent hadronic interactions is then simulated via a relativistic transport (ART) model [74] which includes baryon-baryon, baryon-meson, meson-meson elastic and inelastic scatterings. Therefore, jet energy loss in cold hadronic matter is automatically included in the AMPT simulation by the ART model.

In this work, we simulate Pb+Pb collisions at 2.76 ATeV using the parameters that have been fitted to describe the soft bulk observables at the LHC energies [65]. Two sets of parton interaction cross sections (1.5 and 0 mb) are used to simulate the jet evolution in the dense partonic matter created in Pb+Pb collisions; these two values are to mimic two different physical scenarios: partonic+hadronic interactions and only hadronic interactions.

## III. NUMERICAL RESULT

To study full jets with the AMPT model, we utilize the standard Fastjet package [76] with the anti- $k_T$  algorithm to reconstruct the full jets from the output of the AMPT simulation. To compare with the measurements by CMS Collaboration, we apply the same kinematics for jet cone sizes, transverse momenta, pseudorapidity cuts, and azimuthal angular cuts when reconstructing full jets and studying transverse momentum imbalance distribution and different contributions to the overall momentum balance of asymmetric dijet events.

We first check the transverse momentum imbalance for asymmetric dijet events from the AMPT model by study-

ing the asymmetry variable  $A_J$  defined as follows:

$$A_J = \frac{p_{T,1} - p_{T,2}}{p_{T,1} + p_{T,2}}, \quad (1)$$

where the subscripts 1 and 2 denote the leading and the subleading jets, respectively. The numerical results from the AMPT model simulation are shown in Fig. 1, compared with the CMS measurements [32]. Here the dijet momentum imbalance  $A_J$  distributions (the event fractions) are plotted as a function of  $A_J$  for PbPb collisions at 2.76 ATeV. We apply the same kinematic cuts as the CMS measurements: the jet cone size  $R = 0.5$ , the leading jet  $p_{T,1} > 120$  GeV/c, the subleading jet  $p_{T,2} > 50$  GeV/c, jet pseudorapidity cut  $|\eta_{1,2}| < 2$ , and the rela-

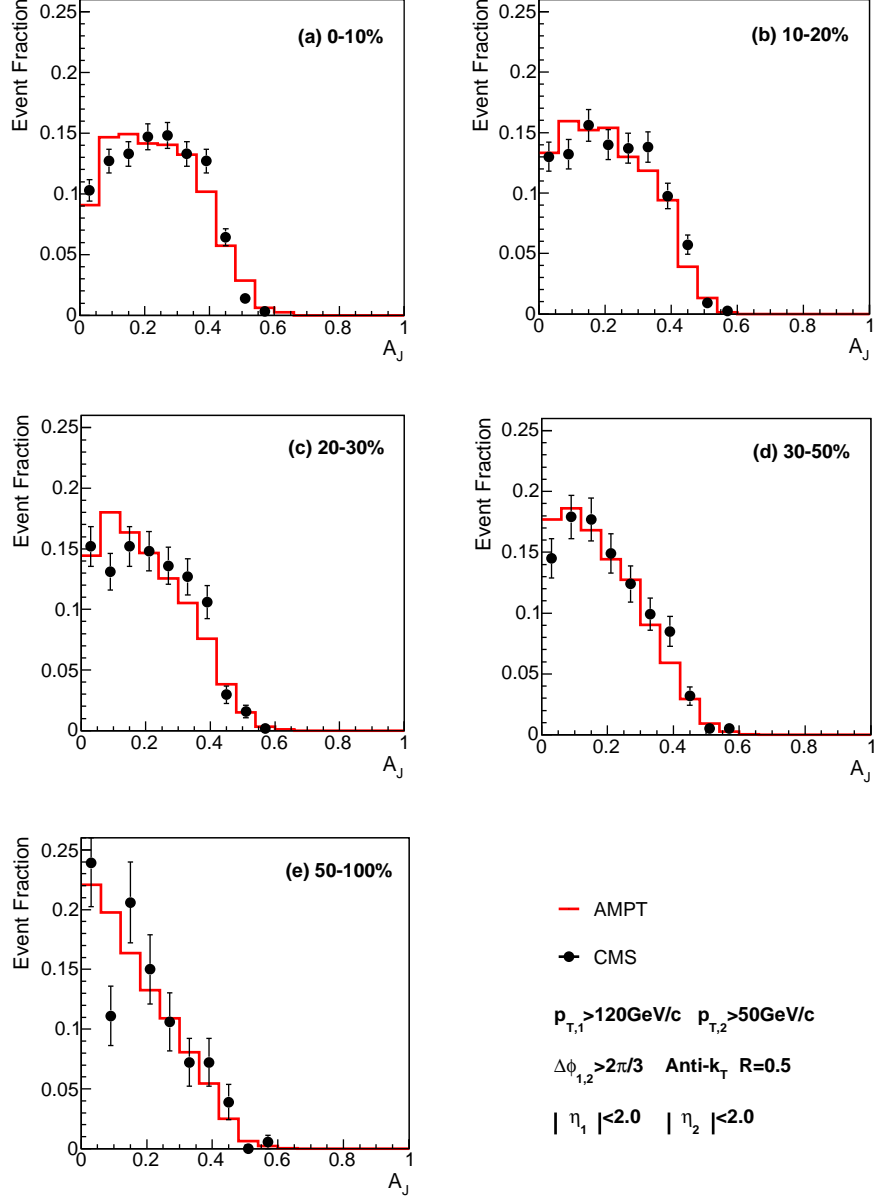


FIG. 1: Dijet  $A_J$  event distributions in 0-10%, 10-20%, 20-30%, 30-50% and 50-100% PbPb collisions at 2.76 ATeV from the AMPT model ( $\sigma = 1.5$  mb), compared to CMS data [32]. The cone size for jet reconstruction is  $R = 0.5$ .

tive azimuthal angle between the leading and subleading jets  $\Delta\phi_{12} = |\phi_1 - \phi_2| > 2\pi/3$ . Five different centrality bins are shown: 0-10%, 10-20%, 20-30%, 30-50%, and 50-100%. To simulate the interactions between the jet and the dense medium, the partonic cross section in the parton cascade is taken to be 1.5 mb in the AMPT model.

From Fig. 1, we can see that from the most peripheral PbPb to the most central PbPb collisions, the dijet momentum imbalance  $A_J$  distribution shifts to the right (i.e., larger  $A_J$  values). This indicates the away-side sub-

leading jets may experience a significant amount of energy loss due to the interactions with the bulk matter produced in PbPb collisions. In central collisions with denser and larger medium, jet-medium interaction is stronger, which leads to larger jet energy loss and thus larger asymmetry  $A_J$ . The result from the AMPT model calculation can quantitatively describe the CMS measurements on dijet  $A_J$  distributions, consistent with a previous study [47].

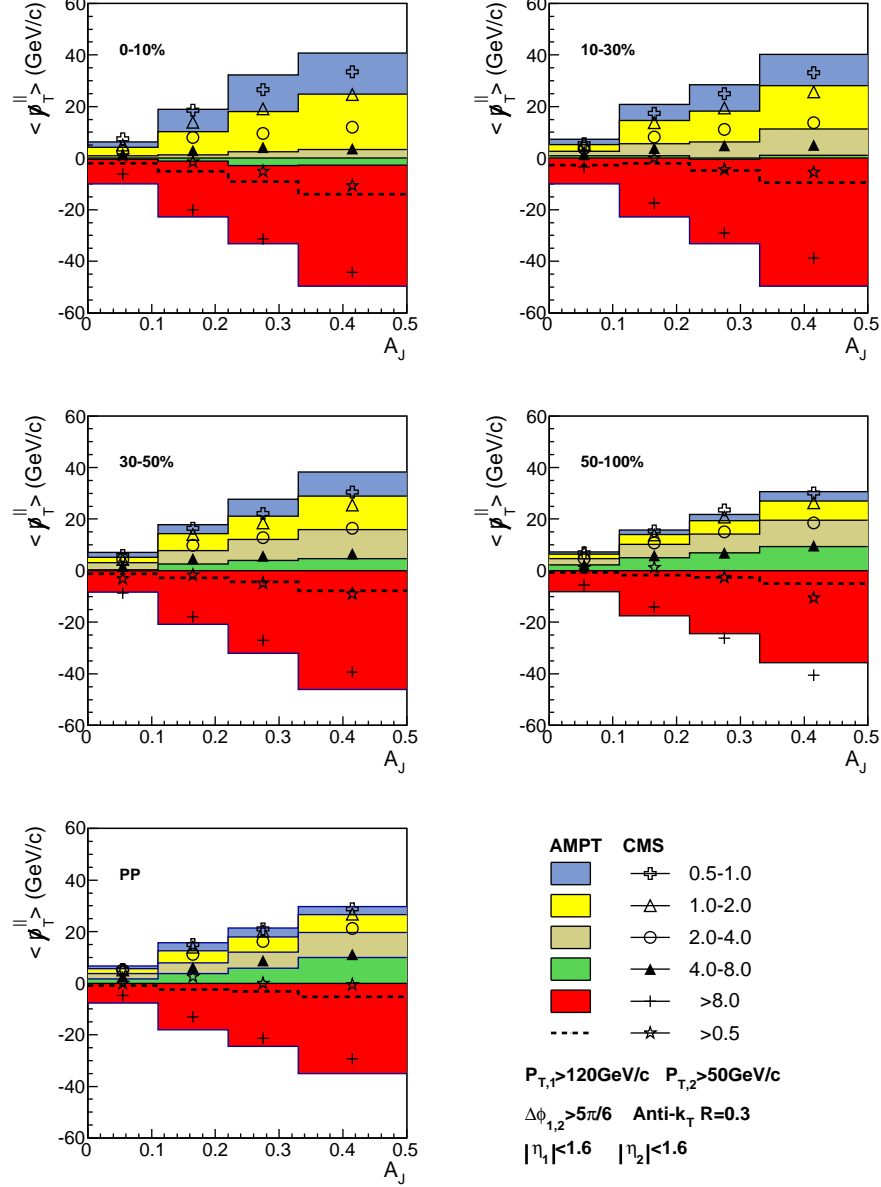


FIG. 2: The event-averaged transverse momentum projection  $\langle p_T^{\parallel} \rangle$  calculated from the AMPT model as a function of  $A_J$  for pp collisions, and 50-100%, 30-50%, 10-30%, 0-10% PbPb collisions at 2.76 ATeV. Each band shows the contribution from charged hadrons with  $p_T = 0.5-1$  GeV/c,  $1-2$  GeV/c,  $2-4$  GeV/c,  $4-8$  GeV/c,  $p_T > 8.0$  GeV/c. The solid lines at the edges of the bands denote the cumulative contributions from different  $p_T$  ranges, and the thick dashed line denotes the cumulative contribution from charged hadrons with  $p_T > 0.5$  GeV/c. The symbols represent the CMS data [75] for cumulative contributions from different  $p_T$  ranges (to be compared to the corresponding lines calculated from the AMPT model). The cone size for jet reconstruction is  $R = 0.3$ .

To further investigate where the lost energy from hard jets goes and how it is redistributed, we follow CMS collaboration [32] and study the overall momentum balance for asymmetric dijet events. One can project the transverse momenta  $p_T$  of all the final charged hadrons onto the leading jet axis, i.e., for each event, the projected

transverse momentum  $p_T^{\parallel}$  can be defined:

$$p_T^{\parallel} = \sum_i -p_T^i \cos(\phi_i - \phi_{\text{leading jet}}), \quad (2)$$

where we take the sum over all final charged hadrons with transverse momenta  $p_T > 0.5$  GeV/c and pseudo-

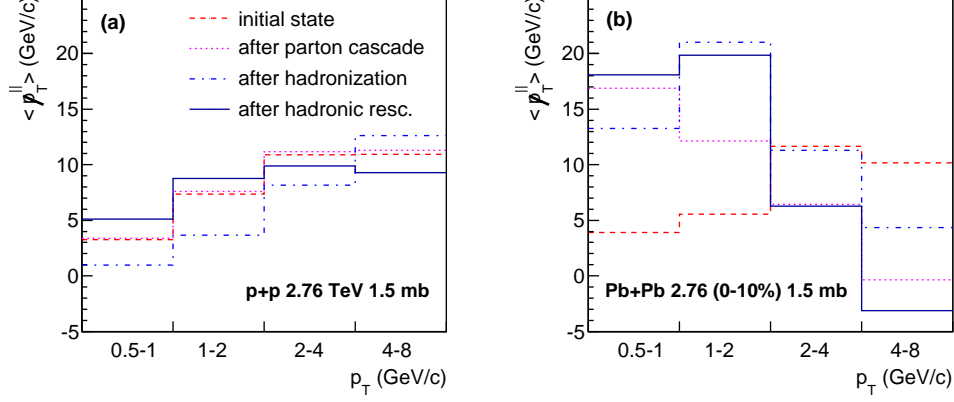


FIG. 3:  $\langle p_T^{\parallel} \rangle$  as a function of  $p_T$  bin in different evolution stages for pp (left) and 0-10% PbPb (right) collisions at 2.76 ATeV calculated from the AMPT model with the partonic interactions.

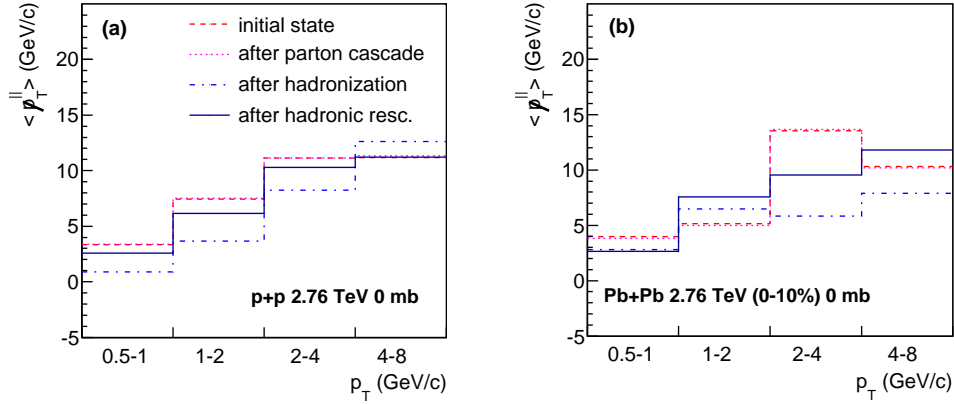


FIG. 4: Same as Fig. 3 but without the partonic interactions.

rapidity  $|\eta| < 2.4$  in following calculations. We then average over the transverse momentum projection  $p_T^{\parallel}$  over all simulated events for given  $A_J$  bins. According to the definition, the negative  $\langle p_T^{\parallel} \rangle$  denotes the projection of the transverse momentum in the direction of the leading jets, while the positive  $\langle p_T^{\parallel} \rangle$  represents the projection in the opposite direction of the leading jets.

The numerical results from the AMPT model calculation are shown in Fig. 2, where the event-averaged transverse momentum projection  $\langle p_T^{\parallel} \rangle$  is plotted as a function of the asymmetry variable  $A_J$  for both pp and PbPb collisions at 2.76 TeV. We use the same kinematics as CMS Collaboration: the jet cone size  $R = 0.3$ , the leading jet  $p_{T,1} > 120$  GeV/c, the subleading jet  $p_{T,2} > 50$  GeV/c, the pseudorapidity cut  $|\eta_{1,2}| < 1.6$ , and the azimuthal angle cut  $\Delta\phi_{12} > 5\pi/6$ . Four different centrality bins are shown: 0-10%, 10-30%, 30-50% and 50-100%. For each centrality bin, we show the individual contributions to the projected transverse momentum  $\langle p_T^{\parallel} \rangle$  from five different  $p_T$  regions: 0.5-1.0 GeV/c, 1.0-2.0 GeV/c, 2.0-

4.0 GeV/c, 4.0-8.0 GeV/c and  $p_T > 8.0$  GeV/c (which are denoted by different bands, respectively, in each plot). The solid curves at the edges of the bands show the cumulative contributions from the combinations of different  $p_T$  bins, and the thick dashed curves denotes the total contribution from the sum of all charged hadrons with  $p_T > 0.5$  GeV/c. The experimental data from CMS measurements are denoted by different symbols, which are then compared to the cumulative contributions from different  $p_T$  bins from the AMPT model simulation (as denoted by the edges of the bands).

From Fig. 2, we can see that in both pp and PbPb collisions, there is a large negative contribution (i.e., in the direction of the leading jets) to the transverse momentum projection  $\langle p_T^{\parallel} \rangle$ , which is dominated by hard charged hadrons ( $p_T > 8.0$  GeV/c). The imbalance contributed from hard hadrons increases from peripheral to central PbPb collisions, which might indicate that the subleading jets tend to hadronize into less hard fragments due to stronger jet-medium interaction and energy loss, as

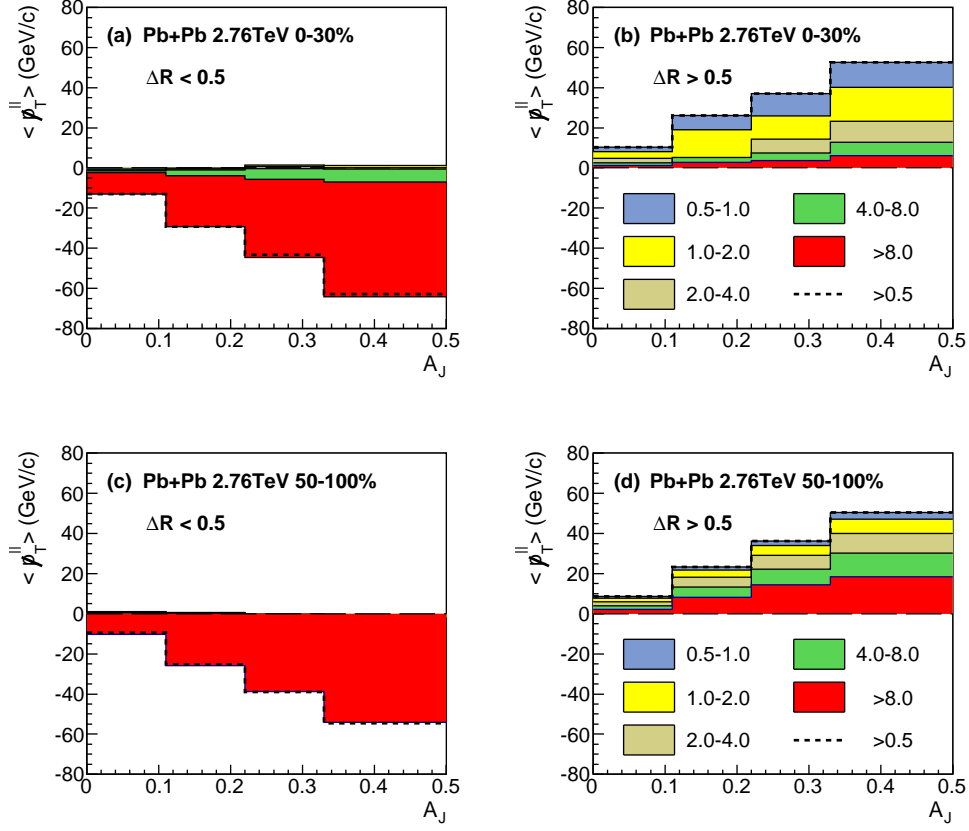


FIG. 5: The in-cone (left) and out-of-cone (right) contributions to the event-averaged transverse momentum projection  $\langle p_T^{\parallel} \rangle$  as a function of  $A_J$  in 0-30% (upper) and 50-100% (lower) PbPb collisions at 2.76 ATeV calculated from the AMPT model. The cone size is 0.5.

compared to the leading jets. Such negative contribution from hard hadrons is mostly balanced by the combined positive contributions from the hadrons with  $p_T = 0.5$ -8 GeV/c. Therefore, the overall projected transverse momentum  $\langle p_T^{\parallel} \rangle_{\text{total}}$  with all hadrons with  $p_T > 0.5$  GeV/c is roughly balanced in both pp and PbPb collisions, as required by the momentum conservation. Of course, due to the kinematic cuts applied on the transverse momentum ( $p_T > 0.5$  GeV/c), the pseudorapidity ( $|\eta| < 2.4$ ), etc., there is still some remaining transverse momentum imbalance after taking into account all the charged hadrons with  $p_T > 0.5$  GeV/c (shown by dashed curves).

Another important observation is that from pp (or peripheral PbPb) to central PbPb collisions, the positive contribution (in the opposite direction of the leading jets) to the projected transverse momentum  $\langle p_T^{\parallel} \rangle$  from the soft hadrons ( $p_T = 0.5$ -2.0 GeV/c) gradually increases and finally dominates in the most central PbPb collisions. This implies that a large portion of the lost energy from the jets is carried by the final state soft hadrons. Since only elastic processes are included in the AMPT model, this implies that the transportation of the lost energy from hard jets into the soft hadrons are mainly caused by

elastic scatterings. Compared to CMS data, the AMPT model can describe quite well the measurements on the overall momentum balance in asymmetric dijet events for both pp and peripheral PbPb collisions. For more central PbPb collisions, AMPT can also give a qualitative description, especially the centrality dependence of the positive contribution from soft hadrons to the transverse momentum projection  $\langle p_T^{\parallel} \rangle$ .

To trace back how the difference on the overall momentum balance for asymmetric dijet events in pp collisions and central PbPb collisions is developed, we calculate the positive contributions to the projected transverse momentum  $\langle p_T^{\parallel} \rangle$  for four different evolution stages in the AMPT model: (i) initial state jet production from HIJING, (ii) after parton cascade, (iii) after hadronization, (iv) after hadron rescattering. The numerical result is shown in Fig. 3, where  $\langle p_T^{\parallel} \rangle$  for charged hadrons with  $p_T = 0.5$ -8.0 GeV/c is plotted as a function of  $p_T$  bin for both pp and central PbPb collisions. For this figure, the dijet asymmetry is taken as  $A_J > 0.15$ ; the results for other  $A_J$  bins are similar. One can see that in central PbPb collisions, the relative contributions from different  $p_T$  hadrons to the transverse momentum projection



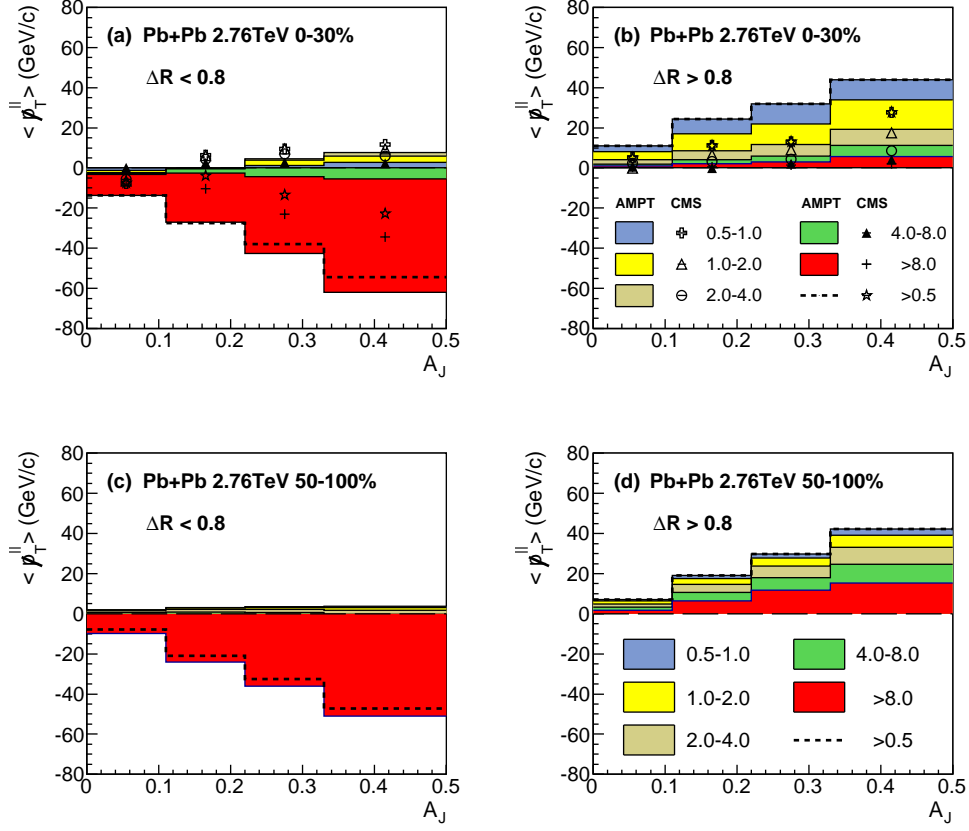


FIG. 6: Same as Fig. 5 but for cone size 0.8. The CMS data is from the reference [32].

$\langle p_T^{\parallel} \rangle$  changes dramatically after parton cascade, in contrast to the result in pp collisions. The hadronization and hadronic interaction also give a visible contribution though not so dramatic as the partonic interaction.

To confirm that the increasing positive contribution from the soft hadrons to the transverse momentum projection  $\langle p_T^{\parallel} \rangle$  is indeed developed in the partonic interaction, we shown in Fig. 4 the projected transverse momentum  $\langle p_T^{\parallel} \rangle$  for charged hadrons with  $p_T = 0.5-8.0$  GeV/c by turning off the partonic interactions in the AMPT model (the partonic cross section is set to be 0 mb). One can see that without partonic interactions, the result from central PbPb collisions is very similar to pp collisions. This implies that the dijet asymmetry is mainly due to jet-medium interactions and jet energy loss in the partonic phase, and the lost energy from the jets is carried by the partons which are fragmented into final state soft hadrons.

Following CMS Collaboration, we further study the angular (re)distribution of the lost energy (carried by the final state soft hadrons) by dividing the total contributions to the projected transverse momentum  $\langle p_T^{\parallel} \rangle$  into two angular regions: one from the charged hadrons inside the cone  $\Delta R = \sqrt{(\phi - \phi_J)^2 + (\eta - \eta_J)^2}$  around the

leading jet axis or the opposite direction, the other is outside the cone  $\Delta R$ , where  $\phi$  and  $\eta$  are the azimuthal angle and pseudorapidity of the charged hadrons, and  $\phi_J$  and  $\eta_J$  are the azimuthal angle and pseudorapidity of the leading jet or sub-leading jet, respectively. From the definition, one knows that with the increasing of the cone size  $\Delta R$ , more hadrons is included in the in-cone contribution (excluded from the out-of-cone contribution). For very large  $\Delta R$ , one includes all charged hadrons in the cones, then the in-cone contribution reduces to the result in Fig. 2.

In Fig. 5, 6 and 7, we show the numerical results the in-cone (left) and out-of-cone (right) contributions to the event-averaged transverse momentum projections  $\langle p_T^{\parallel} \rangle$  as a function of the asymmetry variable  $A_J$ , for central (upper) and peripheral (lower) PbPb collisions at 2.76 ATeV, and for three different cone sizes  $\Delta R = 0.5, 0.8$  and  $1.2$ , respectively. One can clearly see that in both central and peripheral PbPb collisions, and also for three different cone size  $\Delta R$  values, the in-cone contribution to the projected transverse momentum  $\langle p_T^{\parallel} \rangle$  is dominated by large  $p_T$  hadrons ( $p_T > 8.0$  GeV/c) which come from the hard fragments of the reconstructed leading and sub-leading jets. The soft hadrons give quite small in-cone contribution, but the contribution increases when mov-

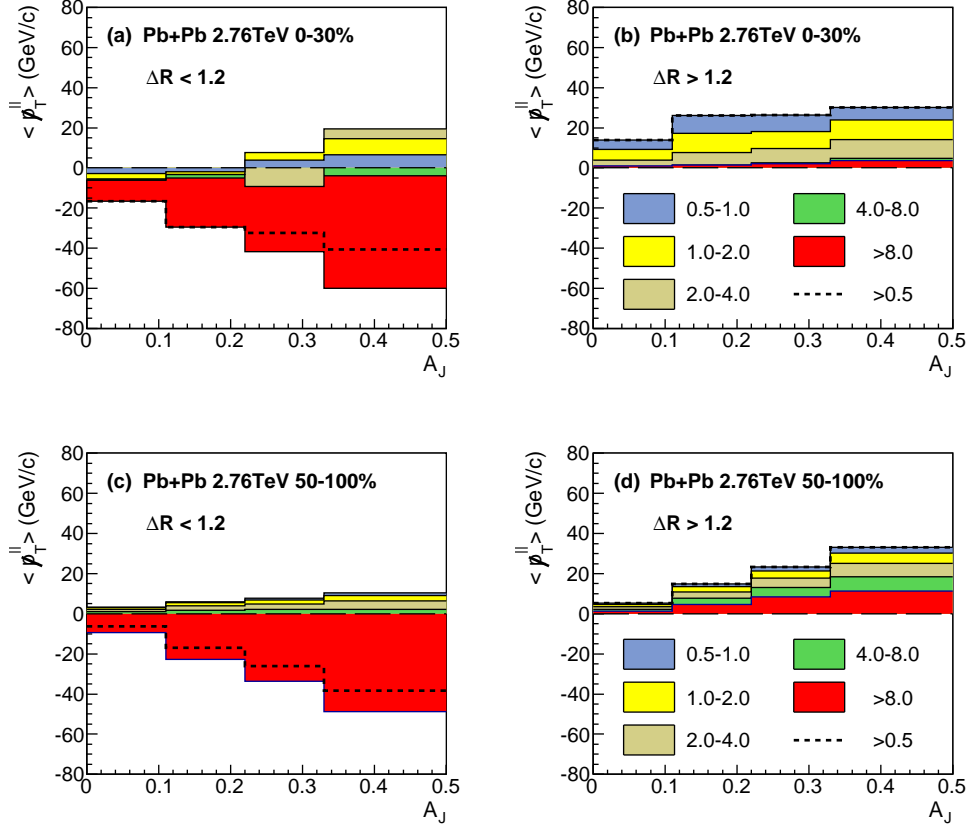


FIG. 7: Same as Fig. 5 but for cone size 1.2.

ing from peripheral to central PbPb collisions or increasing the cone size  $\Delta R$ . For the out-of-cone contribution to  $\langle p_T^{\parallel} \rangle$ , we can see that for peripheral PbPb collisions, there is still a sizable contribution from large  $p_T$  hadrons to  $\langle p_T^{\parallel} \rangle$ . However, for central PbPb collisions, the out-of-cone contribution becomes more dominated by the soft hadrons ( $p_T = 0.5 - 2.0$  GeV/c). This tells that a large fraction of the momentum imbalance (mostly originating from jet-medium interactions and jet energy loss in the partonic stage) in asymmetric dijet events is balanced by the soft hadrons at large angles away from the dijet axis. Noting that the AMPT model only includes elastic processes in the parton cascade, we can conclude that the redistribution of the lost energy from hard jets from our calculation is mainly caused by the elastic collisions which scatterers the relatively soft partons into large angles away from the dijet axis.

In addition, it is interesting to observe that compared to CMS data in Fig. 6, the AMPT simulation somehow overestimates the individual positive and negative contributions to the overall transverse momentum balance. A possible reason for the overestimation might be due to the neglect of the radiative processes in the parton cascade in the AMPT model, which means that we have included more contributions from elastic collisions

in the simulation than the case when radiative processes are included (for similar amount of jet energy loss and dijet asymmetry). Considering that elastic scatterings might be more effective in transporting the momentum to the transverse directions than medium-induced radiation (which is more contributed from collinear radiation), a larger amount of the lost energy from hard jets are transported (by elastic scatterings) to final state soft hadrons at large angles with respect to the jet axis. Future study utilizing the model which includes the both radiative and collisional processes should be helpful to clarify such an issue, which we leave as a future effort.

#### IV. SUMMARY

Within the framework of the AMPT model, we have studied the overall transverse momentum balance and the redistribution of the lost energy from hard jets for asymmetric dijet events in PbPb (and pp) collisions at 2.76 ATeV at the LHC. In particular, we have performed a detailed analysis on the projected transverse momentum  $\langle p_T^{\parallel} \rangle$  contributed from the final-state charged hadrons which carry different transverse momenta and are emitted at different angular directions with respect



to the dijet axis.

For the overall transverse momentum balance, we found that the large negative contribution in the direction of the leading jets to the projected transverse momentum  $\langle p_T^\parallel \rangle$  is dominated by hard hadrons ( $p_T > 8.0$  GeV/c) for both peripheral and central PbPb collisions. In contrast, soft hadrons ( $p_T = 0.5$ -2.0 GeV/c) contributes to positive  $\langle p_T^\parallel \rangle$ . The positive contribution from soft hadrons increases with increasing collision centrality, and dominates in the most central PbPb collisions. This suggests that a large fraction of the lost energy from hard jets is carried by the final state soft hadrons. We have further calculated the positive contributions to  $\langle p_T^\parallel \rangle$  in each evolution stage in the AMPT model which showed that the increasing soft-hadron contribution is indeed developed in the parton cascade, and elastic collisions can effectively transport the lost energy from jets to partons which are fragmented into soft hadrons.

We have also investigated the redistribution of the lost energy in the angular direction by dividing the overall momentum balance into in-cone and out-of-cone contributions relative to the dijet axis. It was found that the in-cone contribution to the projected transverse momentum  $\langle p_T^\parallel \rangle$  is dominated by large  $p_T$  hadrons ( $p_T > 8.0$  GeV/c) in both central and peripheral PbPb collisions, also for three different cone sizes ( $\Delta R = 0.5, 0.8, 1.2$ ). For the out-of-cone contribution to  $\langle p_T^\parallel \rangle$ , while there is still a sizable contribution from large  $p_T$  hadrons in peripheral PbPb collisions, soft hadrons dominate in the most central PbPb collisions. Our result implies that a large amount of the lost energy from hard jets due to jet-

medium interactions (i.e., elastic collisions in the partonic stage in the AMPT model) is transported into the soft partons at large angles away from the dijet direction.

The present study constitutes an important contribution to our understanding of the interaction between hard jets and medium. In particular, we have investigated where the lost energy from hard jets go and how the lost energy is transported during the evolution and is redistributed in the final state hadrons carrying different transverse momenta and emitted at different angles. Our numerical result tends to indicate that elastic collisions in the AMPT model are quite effective in transporting the lost energy from hard jets into large angles with respect to the jet propagation direction. Future studies with the inclusion of and the comparison with the radiative processes will provide a more confirmative information on this issue, e.g., how the medium-induced radiation contributes to the soft hadron production at large angles away from the jet axis. This is left as a future study.

## V. ACKNOWLEDGMENTS

This work was supported by the Natural Science Foundation of China (NSFC) under Grant No. 11435004 and No. 11375072, and by the Major State Basic Research Development Program in China under Grant No. 2014CB845400. G.-L. Ma is supported by NSFC under Grants No. 11522547, No. 11375251, and No. 11421505, and by the Youth Innovation Promotion Association of CAS under Grant No. 2013175.

- 
- [1] X.-N. Wang and M. Gyulassy, Phys.Rev.Lett. **68**, 1480 (1992).
  - [2] G.-Y. Qin and X.-N. Wang, Int. J. Mod. Phys. **E24**, 1530014 (2015), arXiv:1511.00790.
  - [3] STAR, J. Adams *et al.*, Phys. Rev. Lett. **91**, 072304 (2003), arXiv:nucl-ex/0306024.
  - [4] STAR, J. Adams *et al.*, Phys. Rev. Lett. **91**, 172302 (2003), arXiv:nucl-ex/0305015.
  - [5] PHENIX, S. S. Adler *et al.*, Phys. Rev. Lett. **91**, 072301 (2003), arXiv:nucl-ex/0304022.
  - [6] CMS, S. Chatrchyan *et al.*, Eur. Phys. J. **C72**, 1945 (2012), arXiv:1202.2554.
  - [7] ALICE, B. Abelev *et al.*, Phys. Lett. **B720**, 52 (2013), arXiv:1208.2711.
  - [8] STAR, C. Adler *et al.*, Phys. Rev. Lett. **90**, 082302 (2003), arXiv:nucl-ex/0210033.
  - [9] ALICE, K. Aamodt *et al.*, Phys. Rev. Lett. **108**, 092301 (2012), arXiv:1110.0121.
  - [10] PHENIX Collaboration, A. Adare *et al.*, Phys.Rev. **C80**, 024908 (2009), arXiv:0903.3399.
  - [11] STAR Collaboration, B. Abelev *et al.*, Phys.Rev. **C82**, 034909 (2010), arXiv:0912.1871.
  - [12] I. Vitev and M. Gyulassy, Phys. Rev. Lett. **89**, 252301 (2002), arXiv:hep-ph/0209161.
  - [13] X.-N. Wang, Phys. Lett. **B595**, 165 (2004), arXiv:nucl-th/0305010.
  - [14] K. J. Eskola, H. Honkanen, C. A. Salgado, and U. A. Wiedemann, Nucl. Phys. **A747**, 511 (2005), arXiv:hep-ph/0406319.
  - [15] T. Renk and K. Eskola, Phys. Rev. **C75**, 054910 (2007), arXiv:hep-ph/0610059.
  - [16] H. Zhang, J. F. Owens, E. Wang, and X.-N. Wang, Phys. Rev. Lett. **98**, 212301 (2007), arXiv:nucl-th/0701045.
  - [17] G.-Y. Qin *et al.*, Phys. Rev. Lett. **100**, 072301 (2008), arXiv:0710.0605.
  - [18] S. A. Bass *et al.*, Phys. Rev. **C79**, 024901 (2009), arXiv:0808.0908.
  - [19] H. Zhang, J. F. Owens, E. Wang, and X.-N. Wang, Phys. Rev. Lett. **103**, 032302 (2009), arXiv:0902.4000.
  - [20] G.-Y. Qin, J. Ruppert, C. Gale, S. Jeon, and G. D. Moore, Phys.Rev. **C80**, 054909 (2009), arXiv:0906.3280.
  - [21] X.-F. Chen, T. Hirano, E. Wang, X.-N. Wang, and H. Zhang, Phys.Rev. **C84**, 034902 (2011), arXiv:1102.5614.
  - [22] A. Majumder and C. Shen, Phys.Rev.Lett. **109**, 202301 (2012), arXiv:1103.0809.

- [23] K. C. Zapp, F. Krauss, and U. A. Wiedemann, JHEP **03**, 080 (2013), arXiv:1212.1599.
- [24] JET, K. M. Burke *et al.*, Phys. Rev. **C90**, 014909 (2014), arXiv:1312.5003.
- [25] C. Andrs, N. Armesto, M. Luzum, C. A. Salgado, and P. Zurita, Eur. Phys. J. **C76**, 475 (2016), arXiv:1606.04837.
- [26] S. Cao, G.-Y. Qin, and S. A. Bass, Phys.Rev. **C88**, 044907 (2013), arXiv:1308.0617.
- [27] STAR, S. Salur, Eur. Phys. J. **C61**, 761 (2009), arXiv:0809.1609.
- [28] STAR, J. Putschke, Eur. Phys. J. **C61**, 629 (2009), arXiv:0809.1419.
- [29] STAR, E. Bruna, Nucl. Phys. **A830**, 267c (2009), arXiv:0907.4788.
- [30] STAR Collaboration, M. Ploskon, Nucl.Phys. **A830**, 255C (2009), arXiv:0908.1799.
- [31] ATLAS, G. Aad *et al.*, Phys. Rev. Lett. **114**, 072302 (2015), arXiv:1411.2357.
- [32] CMS, S. Chatrchyan *et al.*, Phys. Rev. **C84**, 024906 (2011), arXiv:1102.1957.
- [33] Atlas Collaboration, G. Aad *et al.*, Phys.Rev.Lett. **105**, 252303 (2010), arXiv:1011.6182.
- [34] STAR, P. M. Jacobs and A. Schmah, (2015), arXiv:1512.08784.
- [35] ALICE, J. Adam *et al.*, JHEP **09**, 170 (2015), arXiv:1506.03984.
- [36] CMS Collaboration, S. Chatrchyan *et al.*, JHEP **1210**, 087 (2012), arXiv:1205.5872.
- [37] CMS Collaboration, S. Chatrchyan *et al.*, Phys.Lett. **B730**, 243 (2014), arXiv:1310.0878.
- [38] ATLAS, G. Aad *et al.*, Phys. Lett. **B739**, 320 (2014), arXiv:1406.2979.
- [39] G.-Y. Qin and B. Muller, Phys. Rev. Lett. **106**, 162302 (2011), arXiv:1012.5280, [Erratum: Phys. Rev. Lett.108,189904(2012)].
- [40] J. Casalderrey-Solana, J. G. Milhano, and U. A. Wiedemann, J. Phys. **G38**, 035006 (2011), arXiv:1012.0745.
- [41] I. Vitev and B.-W. Zhang, Phys.Rev.Lett. **104**, 132001 (2010), arXiv:0910.1090.
- [42] C. Young, B. Schenke, S. Jeon, and C. Gale, Phys.Rev. **C84**, 024907 (2011), arXiv:1103.5769.
- [43] Y. He, I. Vitev, and B.-W. Zhang, Phys.Lett. **B713**, 224 (2012), arXiv:1105.2566.
- [44] W. Dai, I. Vitev, and B.-W. Zhang, Phys. Rev. Lett. **110**, 142001 (2013), arXiv:1207.5177.
- [45] G.-Y. Qin, Eur.Phys.J. **C74**, 2959 (2014), arXiv:1210.6610.
- [46] X.-N. Wang and Y. Zhu, Phys.Rev.Lett. **111**, 062301 (2013), arXiv:1302.5874.
- [47] G.-L. Ma, Phys. Rev. **C87**, 064901 (2013), arXiv:1304.2841.
- [48] J. Casalderrey-Solana, Y. Mehtar-Tani, C. A. Salgado, and K. Tywoniuk, Phys.Lett. **B725**, 357 (2013), arXiv:1210.7765.
- [49] J.-P. Blaizot, E. Iancu, and Y. Mehtar-Tani, Phys.Rev.Lett. **111**, 052001 (2013), arXiv:1301.6102.
- [50] L. Fister and E. Iancu, JHEP **03**, 082 (2015), arXiv:1409.2010.
- [51] Y.-T. Chien and I. Vitev, (2015), arXiv:1509.07257.
- [52] J. Milhano and K. C. Zapp, Eur. Phys. J. **C76**, 288 (2016), arXiv:1512.08107.
- [53] N.-B. Chang and G.-Y. Qin, (2016), arXiv:1603.01920.
- [54] J. Casalderrey-Solana, D. Gulhan, G. Milhano, D. Pablos, and K. Rajagopal, (2016), arXiv:1609.05842.
- [55] A. H. Mueller, B. Wu, B.-W. Xiao, and F. Yuan, Phys. Lett. **B763**, 208 (2016), arXiv:1604.04250.
- [56] A. H. Mueller, B. Wu, B.-W. Xiao, and F. Yuan, (2016), arXiv:1608.07339.
- [57] L. Chen, G.-Y. Qin, S.-Y. Wei, B.-W. Xiao, and H.-Z. Zhang, (2016), arXiv:1607.01932.
- [58] J. Casalderrey-Solana, E. Shuryak, and D. Teaney, J.Phys.Conf.Ser. **27**, 22 (2005), arXiv:hep-ph/0411315.
- [59] A. K. Chaudhuri and U. Heinz, Phys. Rev. Lett. **97**, 062301 (2006), arXiv:nucl-th/0503028.
- [60] J. Ruppert and B. Muller, Phys.Lett. **B618**, 123 (2005), arXiv:hep-ph/0503158.
- [61] G. Y. Qin, A. Majumder, H. Song, and U. Heinz, Phys. Rev. Lett. **103**, 152303 (2009), arXiv:0903.2255.
- [62] R. B. Neufeld and B. Muller, Phys. Rev. Lett. **103**, 042301 (2009), arXiv:0902.2950.
- [63] Z.-W. Lin, C. M. Ko, B.-A. Li, B. Zhang, and S. Pal, Phys.Rev. **C72**, 064901 (2005), arXiv:nucl-th/0411110.
- [64] Y. Tachibana and T. Hirano, Phys.Rev. **C90**, 021902 (2014), arXiv:1402.6469.
- [65] J. Xu and C. M. Ko, Phys.Rev. **C83**, 034904 (2011), arXiv:1101.2231.
- [66] G.-L. Ma, Phys. Lett. **B724**, 278 (2013), arXiv:1302.5873.
- [67] G.-L. Ma, Phys.Rev. **C88**, 021902 (2013), arXiv:1306.1306.
- [68] G.-L. Ma, Phys. Rev. **C89**, 024902 (2014), arXiv:1309.5555.
- [69] M.-W. Nie and G.-L. Ma, Phys. Rev. **C90**, 014907 (2014), arXiv:1403.0328.
- [70] X.-N. Wang and M. Gyulassy, Phys. Rev. **D44**, 3501 (1991).
- [71] M. Gyulassy and X.-N. Wang, Comput. Phys. Commun. **83**, 307 (1994), arXiv:nucl-th/9502021.
- [72] T. Sjostrand *et al.*, Comput. Phys. Commun. **135**, 238 (2001), arXiv:hep-ph/0010017.
- [73] B. Zhang, Comput.Phys.Comm. **109**, 193 (1998), arXiv:nucl-th/9709009.
- [74] B.-A. Li and C. M. Ko, Phys.Rev. **C52**, 2037 (1995), arXiv:nucl-th/9505016.
- [75] CMS Collaboration, CMS-PAS-HIN-14-010 (2014).
- [76] M. Cacciari, G. P. Salam, and G. Soyez, Eur.Phys.J. **C72**, 1896 (2012), arXiv:1111.6097.